

Research Article

Magnetic Property and Therapeutic Effect of a New Co(II) Complex on Liver Cancer by Regulating the Expression of miRNA31

Zhenshan Guo ¹, Jun Zhen ¹, Zhoujia Yao ¹, Yemeng Wang ¹ and Chenlu Jin ²

¹Department of Hepatobiliary Surgery, Zhuji People's Hospital of Zhejiang Province, Zhuji, Zhejiang, China

²Department of Endocrinology, Zhuji People's Hospital of Zhejiang Province, Zhuji, Zhejiang, China

Correspondence should be addressed to Chenlu Jin; m51514014@stu.ahu.edu.cn

Received 11 May 2021; Revised 17 September 2021; Accepted 5 October 2021; Published 5 November 2021

Academic Editor: Victor Haber Perez

Copyright © 2021 Zhenshan Guo et al. This is an open access article distributed under the Creative Commons Attribution License, which permits unrestricted use, distribution, and reproduction in any medium, provided the original work is properly cited.

Employing the flexible hexacarboxylate ligand of 1,3,5-triazine-2,4,6-triamine hexaacetic acid (H_6TTHA) to assemble with $Co(NO_3)_2 \cdot 6H_2O$, we have acquired a novel coordination compound, i.e., $[Co_2(H_2TTHA)(H_2O)]_n \cdot 6n(H_2O)$ (1). The analysis of single X-ray diffraction indicated that the H_2TTHA^{2-} ligand μ_5 -bridges connected the Co(II) ions into a two-dimensional layered architecture. Moreover, the magnetic property of 1 was also investigated between 2 and 300 K under 1000 Oe applied magnetic field. The novel compound's inhibitory activity against the viability of cancer cell was determined through CCK-8 assay, and the expression of miRNA31 in liver cancer cells was detected via the real-time RT-PCR.

1. Introduction

Liver cancer is not only the sixth most prevalent cancer but also the second largest malignant tumor having cancer mortality worldwide. China is a country with a large population as well as a country with liver cancer [1]. About half of the new liver cancer patients in the world each year come from our country. Liver cancer is a serious threat to the health of our people. The poor therapeutic effect of liver cancer is largely due to the fact that the medical profession has not clarified its pathogenesis [2]. Up to now, the mechanism of the emergence and development of the liver cancer has not been completely elucidated.

Recently, metal-organic frameworks (MOFs) are of great importance mainly on account of their broad application prospects being utilized as the solid functional materials in various fields, for instance, gas storage, magnetism, luminescence, catalysis, and nonlinear optics [3–7]. Therefore, the design of MOFs is of significance to their properties. To obtain the MOFs with the desired properties, the prerequisites are the careful choice of central metal ion containing desired coordination geometries and organic ligand having

appropriate coordination positions and symmetries. According to the reported papers of MOFs, most MOFs are on the basis of multicarboxylate ligands and transition metal ions, demonstrating that multicarboxylate ligands possess diversified coordination modes and high affinity to transition metal ions [8–12]. 1,3,5-Triazine-2,4,6-triamine hexaacetic acid (H_6TTHA) has six flexible carboxylate arms and can adopt a variety of conformations and coordination patterns based on the geometric requirements of different metal ions. The self-assembly of the H_6TTHA ligand and Zn(II)/Cd(II)/Cu(III)/Co(II)/rare earth ions has afforded lots of intriguing MOFs with interesting luminescent and magnetic properties [13–15]. In view of the unique structural characteristic and multifunctional coordination sites of the H_6TTHA ligand, in this work, the interaction between Co(II) ions and H_6TTHA was completed under the hydrothermal condition which is expected to synthesize new functional MOFs. Successfully, a novel Co(II) compound, i.e., $[Co_2(H_2TTHA)(H_2O)]_n \cdot 6n(H_2O)$ (1), was obtained. The analysis for the diffraction of a single crystal X-ray suggested that the 1 reveals a two-dimensional layered architecture with two pairs of carboxylate arms in *cis-cis* conformation and the

third carboxylate arm in *cis-trans* conformation. Moreover, the complex 1's magnetic performance and thermal stability were also studied. Furthermore, the compound's treatment activity against liver cancer was investigated, and the detail mechanism was discussed in this research.

2. Experimental

2.1. Materials and Instrumentation. The starting materials except the H₆TTHA ligand were of analytical grade and purchased from the Sigma-Aldrich Company. The ligand of H₆TTHA was generated based on reported literature [16]. Through utilizing the analyzer of elemental Vario EL III, the hydrogen, nitrogen, and carbon elements were analyzed. The PXRD could be analyzed and then recorded with the powder diffractometer of the PANalytical X'Pert Pro utilizing the Cu/K α radiation (with λ of 1.54056 Å) with 0.05° step size. The thermogravimetric analyses were implemented via exploiting the thermoanalyzer of NETSCH STA-449C under the atmosphere of N₂ with 10°C/min rate between 30 and 800°C. The luminescent spectra of 1 and organic ligands were collected on the Edinburgh Analytical instrument FLS920.

2.2. Synthesis of Compound [Co₂(H₂TTHA)(H₂O)]_n·6n(H₂O) (1). The mixture prepared from 0.100 mmol of Co(NO₃)₂·6H₂O, 0.05 mmol of H₆TTHA, 0.2 mmol of NaHCO₃, and 10.0 mL of H₂O was sealed into a stainless steel container with PTFE lining (23 mL) and then this mixture was heated for seventy-two hours at 170°C. The complex 1's purple massive crystals were separated with the yield of 38% according to Co(NO₃)₂·6H₂O after cooling the mixture to environmental temperature at 2°C/min rate. Analysis calculated for 1 (chemical formula: C₁₅H₂₄N₆O₁₈Co₂, formula weight: 694.26): N, 12.10%; H, 3.46%; C, 25.93%. Experimental values: N, 12.13%; H, 3.48%; C, 25.89%.

2.3. X-Ray Crystallography. The data of a single crystal was implemented by the graphite-monochromated Mo-K α radiation (with λ of 0.71073 Å) with the diffractometer of Mercury CCD controlled by computer at 293(2) K. The dual direct approach is applied to solve the compound's architecture utilizing the *ShelxT*, and then, the refinement package of *ShelXL* is utilized to refine this structure via least squares minimization [17]. The complex 1's data of crystallography were detailed and then concluded in Table 1. The chose bond angles (°) and bond lengths (Å) of the complex 1 are revealed in Table S1.

2.4. CCK-8 Assay. The novel compound's inhibitory activity against the liver cancer cell viability was detected through exploiting the CCK-8 assay. This conduction was completed fully based on the protocols' guidance with some modifications. In general, in the stage of logical growth, the liver cancer cells of HepG2 were harvested, and then, they were planted at 1×10^4 /well destiny in 96-well plates. The cells could be inoculated in a 5-percent humidified CO₂ and 37°C incubator. After the liver cancer cells of HepG2 went up to 70-80 percent confluence, the compound (1 μ M,

TABLE 1: The complex 1's crystal data indexes.

Formula	C ₁₅ H ₂₄ N ₆ O ₁₈ Co ₂
Fw	694.26
Crystal system	Orthorhombic
Space group	Pca2 ₁
<i>a</i> (Å)	22.4966 (6)
<i>b</i> (Å)	11.1009 (3)
<i>c</i> (Å)	9.9004 (3)
α (°)	90
β (°)	90
γ (°)	90
Volume (Å ³)	2472.45 (12)
<i>Z</i>	4
Density (calculated)	1.865
Abs. coeff. (mm ⁻¹)	1.441
Total reflections	8970
Unique reflections	3081
Goodness of fit on <i>F</i> ²	1.052
Final <i>R</i> indices (<i>I</i> > 2sigma(<i>I</i> ²))	<i>R</i> = 0.0532, <i>wR</i> ₂ = 0.1494
<i>R</i> (all data)	<i>R</i> = 0.0557, <i>wR</i> ₂ = 0.1531
CCDC	2082854

2 μ M, 4 μ M, 8 μ M, 10 μ M, 20 μ M, 40 μ M, 80 μ M, 100 μ M) was added into a PBS well of the same volume. After treating for twenty-four hours, the medium of the culture was discarded, and then, the cells were washed by utilizing the preclod PBS. Afterwards, the medium with the reagent of CCK-8 (Sigma) was added to each well to incubate for 4 hours in darkness. Ultimately, for each well, its value of optical density (OD) was determined at the 490 nm wavelength. This experiment was implemented for 3 times or more.

2.5. Real-Time RT-PCR. For the sake of detecting the miRNA31 expression in liver cancer cells, after treating via the compound, the real-time RT-PCR was conducted in our experiment. Briefly, in the stage of logical growth, the liver cancer cells of HepG2 were harvested, and then, they were planted at 2×10^5 /well ultimate destiny in 6-well plates. Afterwards, the cells could be inoculated in a 5-percent CO₂ and 37°C incubator overnight. After the cells went up to 75 percent confluence, the compound (10 ng/mL, 20 ng/mL, 50 ng/mL) was added into the well to carry out the treatment for 24 hours. After finishing the indicated treatment, in distinct groups, the cells were collected and the overall RNA could be extracted via exploiting the TRIzol Reagent (Sigma, St. Louis, MO, USA). In accordance with the proposal of manufacturer, the RNA was transcribed reversely into the cDNA by kit. The SYBR Green Master Mix (Roche) was utilized for real-time RT-PCR, and *gapdh* was applied as an internal control to detect the miRNA31 relative expression. The outcomes were acquired via employing the $2^{-\Delta\Delta C_t}$ approach for 3 times.

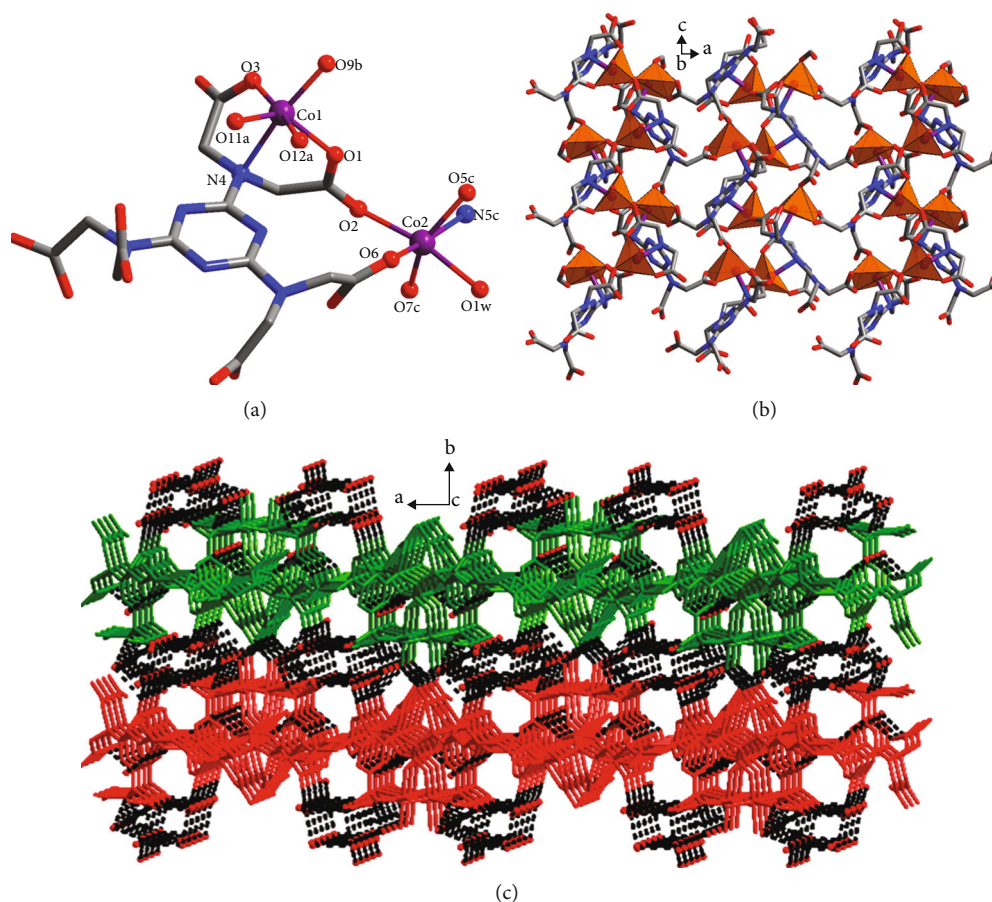


FIGURE 1: (a) The coordination surrounding view of Co(II) ions in the complex 1. (b) The 1's two-dimensional layered architecture. (c) The three-dimensional supramolecular skeleton of complex 1 via the connection of multipoint H bonds (black dotted lines stands for the H bonds).

3. Results and Discussion

3.1. Crystal Structure of Compound 1. The complex 1's architecture was crystallized in the space group of Pca_21 of orthorhombic system. The 1's fundamental unit is constructed from 2 separated Co(II) ions in crystallography, a ligand of H_2TTHA^{4-} , a terminal ligand of water, along with 5 lattice molecules of water. As reflected in Figure 1(a), the Co1 ion exhibits a hexacoordinated geometry of octahedron defined through 5 carboxylic acid O atoms (i.e., O9b, O12a, O11a, O3, and O1) along with a N atom (namely, N4) derived from 3 diverse ligands of H_2TTHA^{4-} , and the Co2 ion also displays a six-coordinated octahedral geometry surrounded by one terminal water ligand, 4 carboxylic acid O atoms (i.e., O7c, O5c, O6, and O2), and a N atom (N5c) comes from two separate H_2TTHA^{4-} ligands. The distance of Co-O is between 1.984(8) and 2.188(7) Å, and the length of Co-N is between 2.398(8) and 2.400(8) Å, respectively, which are comparable with those coordination polymers based on the similar organic ligands such as $\{[Co_{1.5}(TBIP)_{1.5}(L)] \cdot 0.5-H_2O\}_n$ (Co-O/N: 1.973(2) to 2.359(2) Å) [18] and $\{[Co(L)]_2\}_n \cdot nCH_3COCH_3$ (Co-O/N: 1.976(2) to 2.449(2) Å) [19]. The polycarboxylate H_6TTHA ligand is incompletely deprotonated into the form of H_2TTHA^{4-} that utilizes as a

μ_5 -bridge linking 5 diverse Co(II) ions, and the specific coordination pattern of H_2TTHA^{4-} is revealed in Figure S1. It is noteworthy that two pairs of carboxylate groups are in *cis-cis* conformation, and the third pair of carboxylate group is in *cis-trans* conformation. Consequently, all the Co(II) ions are linked together through the carboxylic acid groups from the H_2TTHA^{4-} ligands with six flexible arms, affording a 2D layered structure extending along the crystallographic *bc* plane. The structure of 1 contains lots of carboxylic acid groups, the lattice, and coordinated molecules of water. Thus, there exist abundant hydrogen bond interactions between carboxylic acid O atoms, coordinated molecules of water, lattice molecules of water and coordinated molecules of water, lattice water molecules and lattice water molecules, and carboxylic acid O atoms and lattice molecules of water, and the detailed parameters of the H-bond are revealed in Table S2. In the end, these interactions of hydrogen in-depth linked neighboring two-dimensional layers into a three-dimensional supramolecular skeleton (Figure 1(c)).

3.2. Powder X-Ray Diffraction Pattern (PXRD) and Thermogravimetric Analysis (TGA). The bulk samples' phase purity is demonstrated though the patterns of PXRD

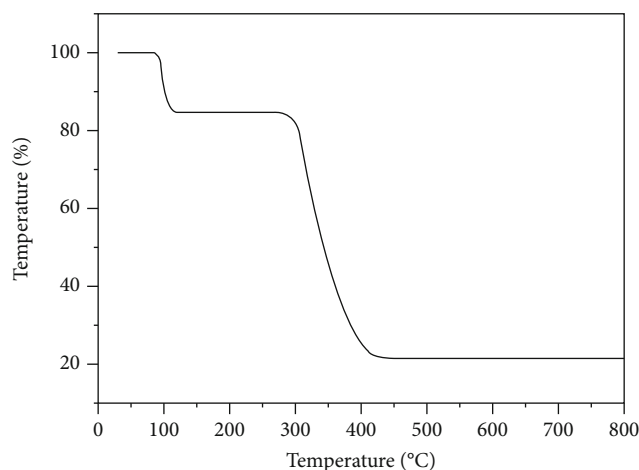


FIGURE 2: The TGA curve of 1.

reflected in Figure S2. For the simulated pattern, the diffraction peaks are in accordance with the experiment results, and this reflects that the bulk samples are in the single phase.

Furthermore, we also investigated the 1's thermal behavior under nitrogen atmosphere from 30-800°C, and the TGA curve is plotted in Figure 2. It can be observed that the framework of 1 experienced a two-step process of weightlessness. The first 15.48% of weightlessness appeared between 83 and 116°C, which is on account of the loss of the coordinated and lattice molecules (with the calculated value of 15.56%), and the second step accompanied by rapid and significant weight loss occurred from 277°C and ended at 421°C, leaving the final residues of 21.42% corresponding to the generation of CoO (calculated: 21.59%).

3.3. Magnetic Property of 1. The complex 1's magnetic susceptibility with temperature was determined in 1000 Oe external magnetic field ranging from 2 K to 300 K. In accordance with the plot of T vs. $\chi_M T$ which is reflected in Figure 3, it can be observed that at 300 K, the $\chi_M T$ value is $2.75 \text{ cm}^3 \cdot \text{mol}^{-1} \cdot \text{K}$, which is greater than the pure spin value (namely, $1.87 \text{ cm}^3 \cdot \text{mol}^{-1} \cdot \text{K}$) for the Co(II) ion with a high-spin value ($g = 2.0$ and $S = 3/2$). Such a higher value is caused by the contribution of orbital angular momentum to the magnetic susceptibility at a high temperature [20]. With the decrease of temperature, the $\chi_M T$ value monotonically reduces, and the minimum value is $0.82 \text{ cm}^3 \cdot \text{mol}^{-1} \cdot \text{K}$, suggesting that between the Co(II) ions, there exist weak antiferromagnetic interactions. The plot of T vs. $1/\chi_M$ exhibits the linear relationship between 50 and 300 K and adheres to the law of Curie-Weiss, and the Curie constant of C and Weiss constant of θ is $2.86 \text{ cm}^3 \cdot \text{mol}^{-1} \cdot \text{K}$ and -2.67 K , respectively. For the Weiss constant, its negative value in-depth proves that between the Co(II) ions, there is an antiferromagnetic interaction [21–23].

3.4. Compound Significantly Reduces the Viability of the Cancer Cells. After creating the novel compound, the assessment of bioactivity on liver cancer cells was conducted. As a

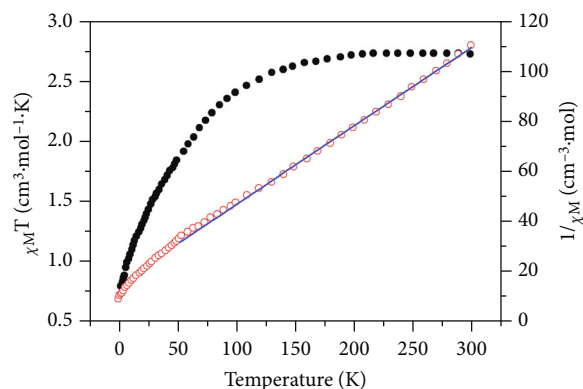
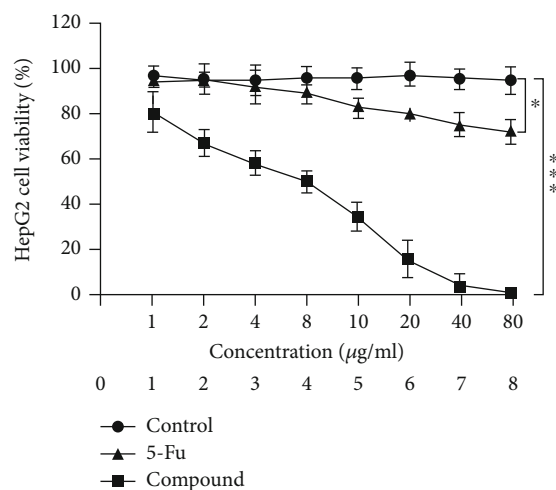
FIGURE 3: The 1's temperature dependence of $1/\chi_M$ and $\chi_M T$.

FIGURE 4: Significantly reduced the cancer cell viability after treating through the compound. Positive drug, 5-Fu, and the prepared fresh compound could be employed for the treatment of liver cancer cells. The CCK-8 assay was carried out, and the novel compound's viability was detected.

result, the CCK-8 assay was implemented, and the liver cancer cell viability was detected. As per the outcomes illustrated in Figure 4, the cancer cell viability could be remarkably decreased by compound in contrast to the control group. The novel compound's inhibition was even much stronger than the positive drug, 5-Fu.

3.5. Compound Obviously Inhibited the Expression of miRNA31 in the Liver Cancer Cells. In the above results, we can see that the compound was good at inhibiting the cancer cell viability, as the miRNA31 expression in liver cancer cells possesses an essential effect in the viability of cell. Thus, the real-time RT-PCR was accomplished, and the miRNA31 expression in liver cancer cells was determined. The outcomes in Figure 5 suggested that in comparison with the control group, the model group has a higher expression level of miRNA31 in the liver cancer cells. The compound obviously reduced the miRNA31 relative expression in liver cancer cells. This inhibition indicated the time- and dose-dependent relationship.

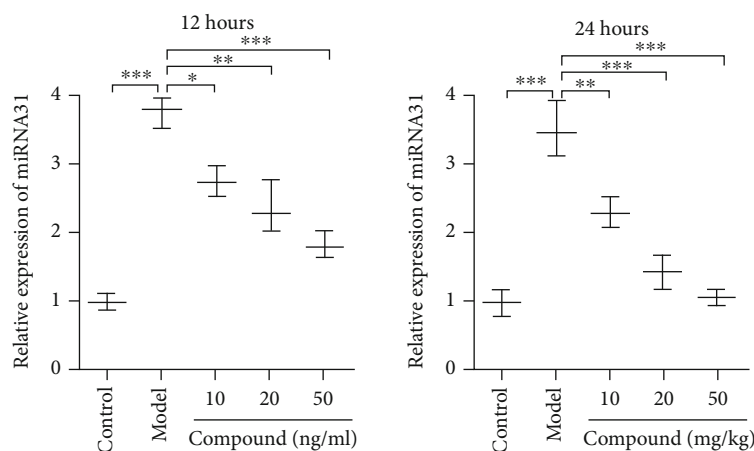


FIGURE 5: Evidently inhibited miRNA31 expression in liver cancer cells after treating with compound. The novel compound was employed to treat liver cancer cells; the miRNA31 expression was detected through the real-time RT-PCR.

4. Conclusion

In summary, one new Co(II) compound was synthesized by using the flexible hexacarboxylate ligand of H6TTHA under hydrothermal conditions. Compound 1 exhibits a two-dimensional layered architecture through the connection of H2TTHA4-ligands with Co(II) ions. It is worth noting that there are rich H-bonds between carboxylic acid O atoms, the lattice molecules of water, and the coordination molecules of water, which in-depth link these two-dimensional layers into the three-dimensional supramolecular skeleton. The variable-temperature magnetic performance researches suggest the complex 1's weak antiferromagnetic behavior. The CCK-8 assay outcomes reflected that this compound could remarkably decrease the cancer cell viability. Besides, the expression of miRNA31 in liver cancer cells was also increased through this compound dose dependently. Ultimately, it can be summed up that the fresh compound could be an outstanding candidate for the liver cancer treatment by regulating the expression of miRNA31 in the liver cancer cells; this result also proved the previous researches [24].

Data Availability

Selected bond lengths (Å) and angles (°) for 1 (Table S1); the detailed hydrogen bond parameters for 1 (Table S2); the detailed coordination mode of H2TTHA4-ligand (Figure S1); the PXRD patterns for 1 (Figure S2), the information could be found in the supporting information file.

Conflicts of Interest

The authors declare that there is no conflict of interest regarding the publication of this paper.

Supplementary Materials

Selected bond lengths (Å) and angles (°) for 1 (Table S1), the detailed hydrogen bond parameters for 1 (Table S2), the detailed coordination mode of H₂TTHA⁴⁻ ligand (Figure S1), and the PXRD patterns for 1 (Figure S2); the

information could be accessed in the supplementary material. (*Supplementary Materials*)

References

- [1] A. Marengo, C. Rosso, and E. Bugianesi, "Liver cancer: connections with obesity, fatty liver, and cirrhosis," *Annual Review of Medicine*, vol. 67, no. 1, pp. 103–117, 2016.
- [2] J. H. Sun, Q. Luo, L. L. Liu, and G. B. Song, "Liver cancer stem cell markers: progression and therapeutic implications," *World Journal of Gastroenterology*, vol. 22, no. 13, pp. 3547–3557, 2016.
- [3] H. Xia, X. Jiang, C. Jiang, and G. Liao, "Two new carboxylate-bridged one-dimensional coordination polymers based on macrocyclic metallic tectons," *Russian Journal of Coordination Chemistry*, vol. 40, no. 2, pp. 93–99, 2014.
- [4] X. Feng, Y. Q. Feng, L. Liu, L. Y. Wang, H. L. Song, and S. W. Ng, "A series of Zn-4f heterometallic coordination polymers and a zinc complex containing a flexible mixed donor dicarboxylate ligand," *Dalton Transactions*, vol. 42, no. 21, pp. 7741–7754, 2013.
- [5] X. Feng, N. Guo, R. F. Li et al., "A facile route for tuning emission and magnetic properties by controlling lanthanide ions in coordination polymers incorporating mixed aromatic carboxylate ligands," *Journal of Solid State Chemistry*, vol. 268, pp. 22–29, 2018.
- [6] M. L. Hu, Y. M. Mohammad, and A. Morsali, "Template strategies with MOFs," *Coordination Chemistry Reviews*, vol. 387, pp. 415–435, 2019.
- [7] M. L. Hu, V. Safarifar, E. Doustkhah et al., "Taking organic reactions over metal-organic frameworks as heterogeneous catalysis," *Microporous and Mesoporous Materials*, vol. 256, pp. 111–127, 2018.
- [8] M. L. Hu, M. Abbasi-Azad, B. Habibi et al., "Electrochemical applications of ferrocene-based coordination polymers," *ChemPlusChem*, vol. 85, no. 11, pp. 2397–2418, 2020.
- [9] L. Fan, D. Zhao, B. Li et al., "Luminescent binuclear Zinc(II) organic framework as bifunctional water-stable chemosensor for efficient detection of antibiotics and Cr(VI) anions in water," *Spectrochimica Acta, Part A: Molecular and Biomolecular Spectroscopy*, vol. 264, article 120232, 2022.

- [10] X. Zhang, Y. Y. Huang, Q. P. Lin, J. Zhang, and Y. G. Yao, "Using alkaline-earth metal ions to tune structural variations of 1,3,5-benzenetricarboxylate coordination polymers," *Dalton Transactions*, vol. 42, no. 6, pp. 2294–2301, 2013.
- [11] L. Feng, F. Ye, X. Ning, M. Zhou, and H. Hou, "Water adsorption and magnetic properties of Mn^{II} -MOFs assembled by triazine-based polycarboxylate and 4, 4'-bipy," *Journal of Solid State Chemistry*, vol. 284, article 121204, 2020.
- [12] L. Y. Wang, X. Han, Z. Shi, Y. H. Xing, and L. X. Sun, "Copper triazine polycarboxylic acid crystalline framework materials: synthesis, structure and multifunctional properties with the luminescent and catalytic reduction of 4-NP," *Polyhedron*, vol. 195, p. 114966, 2021.
- [13] S. Li, J. Song, J. C. Ni et al., "Photoelectric properties and potential nitro derivatives sensing by a highly luminescent of Zn(ii) and cd(ii) metal-organic frameworks assembled by the flexible hexapodal ligand, 1,3,5-triazine-2,4,6-triamine hexaacetic acid," *RSC Advances*, vol. 6, no. 42, pp. 36000–36010, 2016.
- [14] L. Feng, M. Zhou, F. Ye, C. Chen, and H. Hou, "Water adsorption and proton conduction of a cobalt(ii) complex assembled by triazine-based polycarboxylate," *Dalton Transactions*, vol. 48, no. 40, pp. 15192–15197, 2019.
- [15] Q. Zhu, T. Sheng, R. Fu et al., "Syntheses, structural aspects, luminescence and magnetism of four coordination polymers based on a new flexible polycarboxylate," *CrystEngComm*, vol. 13, no. 6, pp. 2096–2105, 2011.
- [16] Q. Zhu, T. Sheng, R. Fu et al., "Novel structures and luminescence properties of lanthanide coordination polymers with a novel flexible polycarboxylate ligand," *Crystal Growth & Design*, vol. 9, no. 12, pp. 5128–5134, 2009.
- [17] G. M. Sheldrick, "Crystal structure refinement with SHELXL," *Acta Crystallographica Section C-Structural Chemistry*, vol. 71, no. 1, pp. 3–8, 2015.
- [18] Q. Q. Xiao, G. Y. Dong, Y. H. Li, and G. H. Cui, "Cobalt(II)-based 3D coordination polymer with unusual 4,4,4-connected topology as a dual-responsive fluorescent Chemosensor for Acetylacetone and $Cr_2O_7^{2-}$," *Inorganic Chemistry*, vol. 58, no. 23, pp. 15696–15699, 2019.
- [19] J. F. Wang, T. Feng, Y. J. Li, Y. X. Sun, W. K. Dong, and Y. J. Ding, "Novel structurally characterized co(II) metal-organic framework and cd(II) coordination polymer self-assembled from a pyridine-terminal Salamo-like ligand bearing various coordination modes," *Journal of Molecular Structure*, vol. 1231, article 129950, 2021.
- [20] G. J. Xu, C. Xu, S. R. Zhang et al., "Controllable synthesis and magnetic properties of two stable cobalt-organic frameworks based on 5-(4-carboxybenzyloxy)isophthalic acid," *Inorganic Chemistry Communications*, vol. 95, pp. 27–31, 2018.
- [21] M. Y. Sun and D. M. Chen, "A rare high-connected metal-organic framework with an unusual topological net: synthesis, crystal structure and magnetic properties," *Inorganic Chemistry Communications*, vol. 82, pp. 61–63, 2017.
- [22] M. X. Zheng, X. J. Gao, C. L. Zhang, L. Qin, and H. G. Zheng, "Assembly of various degrees of interpenetration of co-MOFs based on mononuclear or dinuclear cluster units: magnetic properties and gas adsorption," *Dalton Transactions*, vol. 44, no. 10, pp. 4751–4758, 2015.
- [23] Z. Z. Zhang, G. H. Lee, and C. I. Yang, "The use of a semi-flexible bipyrimidyl ligand for the construction of azide-based coordination polymers: structural diversities and magnetic properties," *Dalton Transactions*, vol. 47, no. 46, pp. 16709–16722, 2018.
- [24] S. Wang, Z. Wang, Q. Wang, Y. Cui, and S. Luo, "Clinical significance of the expression of miRNA-21, miRNA-31 and miRNA-let7 in patients with lung cancer," *Saudi Journal of Biological Sciences*, vol. 26, no. 4, pp. 777–781, 2019.